FORECASTING OF ROLLING MOTION OF SMALL FISHING VESSELS UNDER FISHING OPERATION APPLYING A NON-DETERMINISTIC METHOD

Nobuo Kimura , Kiyoshi Amagai
Graduate School of Fisheries Sciences, Hokkaido University (Japan)

Abstract

This paper concerns with a methodology using a non-deterministic method to express the nonlinear dynamic rolling motion of small fishing vessels. As the rolling response system of the small fishing vessels for the waves is generally indicating strong nonlinearity and the effect of fishing operation for the ship motions is remarkable, proper estimation according to dynamic changes of ship condition is required to improve the safety on the seakeeping qualities. To apply the *Neural Network* model for the actual phenomenon, we have carried out improvements based on the tank tests.

In this paper, main points of the improvements are as follows: (1) the accuracy of the estimation, (2) the selection of proper input for the model and (3) expansion of the framework from the estimation to the forecasting. According to the accuracies on the estimating for the full-scale experiments, we propose the practicability applying the *Neural Network* model to forecast the rolling motion of small fishing vessels under the actual fishing operation conditions.

1. INTRODUCTION

It is well known that strong nonlinear movements frequently emerge on the rolling motion of fishing vessels since complicated forces generated during fishing operation would act the dynamic response system. As majority of fishing vessels are doing fishing operation on the ship side using huge fishing gear, appropriate estimation of the seakeeping quality related to the rolling motion is so important to secure the safety of the fishing vessels. To avoid the instantaneous danger owing to large rolling motion under fishing operation condition, we intend to develop the roller equipments, which are located on a connecting point between the ship and fishing gear, with the autonomous supervising system adjusting the forces due to the fishing operation according to demand. In order to develop such safety system, we should adopt the proper forecasting model for the rolling motion based on the information of actual measurement. Further, decrease of the large rolling motion would be possible if a force controller network adjusting the force of the roller under the fishing operation attached to the forecasting model.

To estimate the dynamic rolling response system of the fishing vessels under the fishing operation, we have studied application of a *Neural Network* model, which is one of the non-deterministic methods [1-5]. In the 7th conference on STAB, based on the results on the estimation for tank tests, we showed the effectiveness of the *Neural Network* model to express the rolling response with the effect of the fishing operation [6-7].

In this paper, to construct a forecasting model, we especially took notice of applying a recurrent *Neural Network* model to the rolling response system under fishing operation. Based on the forecasting with sufficient accuracy, we suggest that the recurrent *Neural Network* model is effective as the forecasting model for the actual rolling motion under the fishing operation.

2. EXPERIMENT

We focused on the small fishing vessel for scallop hanging culture, which is one of the main fishing in *Hokkaido, Japan*. It is one of dangerous fishing since the fishing operation is always doing under mooring condition to the big scale culture facilities on the rough sea. General construction of the facilities of the scallop hanging culture and the fishing operation condition are shown in Fig. 1.

Using two small fishing vessels for the scallop hanging culture, we have conducted the full-scale experiments in *Uchiura-Bay*, *Japan* from October 1999 to March 2001. One fishing vessel was the 7.9 *GT* type, and another was the 6.6 *GT* type. The measured variables were as follows: wave height, the six degrees of freedom of the movements and vertical mooring force for the facilities of the scallop culture. The co-ordinate system of the ship motions is shown in Fig. 2. Time interval between sampling was 0.05 second. The wave height was defined as the relative displacement between the edge of bow ship and the sea surface and it was measured by a wave height meter of the capacity type. High frequency noise was eliminated from measured accelerations, which corresponded to the heaving, surging and swaying motions.

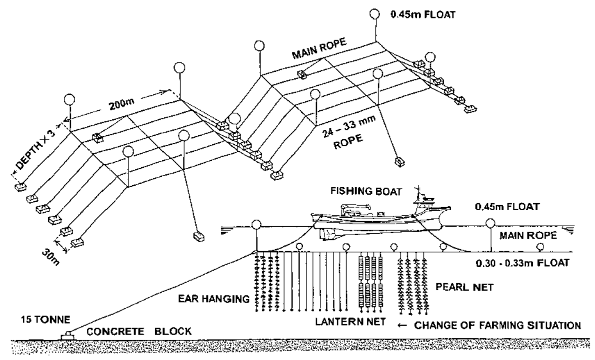

Fig. 1. View of the fishing operation of the fishing vessels for scallop hanging culture

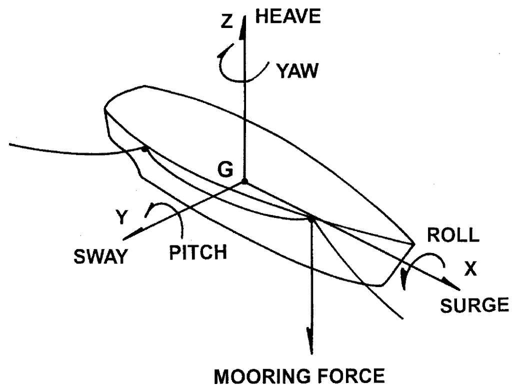

Fig. 2. Co-ordinate system

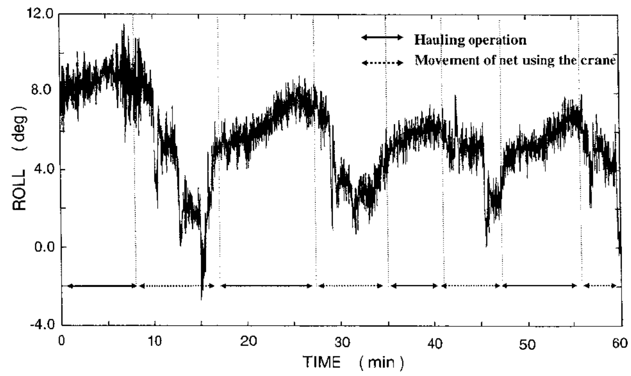

Fig. 3. Time series of the rolling motion of the 7.9 *GT* fishing vessel under the fishing operation

An example of time series of the rolling motion on the 7.9 *GT* fishing vessel under the fishing operation for one hour is shown in Fig. 3. As series of the fishing operation, which fishermen hauled up the lines with scallops onto the deck and moved about 800 kg weight of net stuffed with scallops to the opposite side in order to adjust the heeling angle, were repeated four times, the ship condition was largely changed in a short period.

The principal particulars are shown in Table 1 and the lines are shown in Fig.4 and Fig. 5. Also, the righting lever curves under light load condition are shown in Fig. 6 and Fig. 7, respectively. Considering the large transverse metacentric height $\overline{GM}$ and the righting lever $\overline{GZ}$ shown in the figures, both fishing vessels generally have sufficient static stability until the top of the bulwark will sink under sea level. As most small fishing vessels have relatively high bulwark to make up for the seakeeping quality, the static stability would become worse if the shipping water would happen.

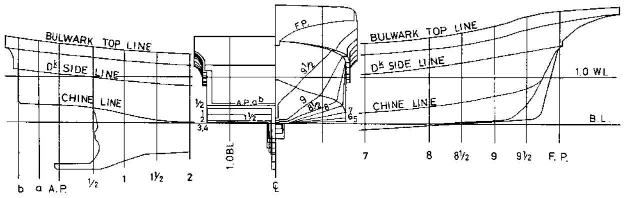

Fig. 4. Lines of the 6.6 *GT* fishing vessel

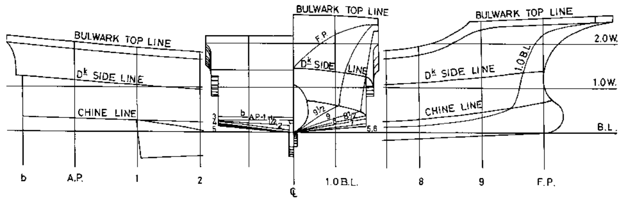

Fig. 5. Lines of the 7.9 *GT* fishing vessel

Table 1. Principal particulars

	7.9 GT type	6.6 GT type
Lpp (m)	14.14	13.21
B (m)	3.63	3.02
D (m)	0.95	0.88
Disp. (ton)	14.77	14.34
dm (m)	0.48	0.45
TRIM (m)	0.20	0.14
KG (m)	0.73	0.93
GM (m)	1.93	1.25
OG (m)	1.03	1.19

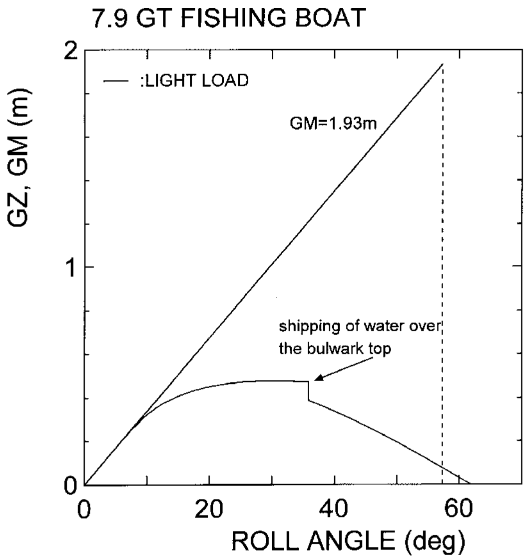

Fig. 6. Stability curve of the 7.9 *GT* fishing vessel

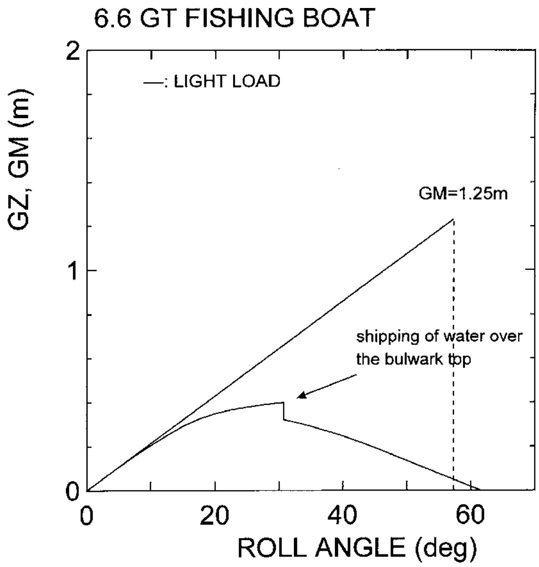

Fig. 7. Stability curve of the 6.6 *GT* fishing vessel

3. METHODOLOGY

3.1. Structural model of the roll response

Schematic diagram of structure of the *Neural Network* model is shown in Fig. 8. A single hidden layer feed-forward *Neural Network* model is applied for the estimation of the rolling motion measured on the full-scale experiments. The model is constructed with three layers: the input layer *I*, the hidden layer *J* and the output layer *K*. The estimated rolling motion $\tilde{R}(t)$ at the time *t* is expressed as the output from the model, and it is written as follows:

$$\tilde{R}(t) = \sum_{j=1}^{M_{hidden}} W_{J_j K_1} f(Y_{J_j}(t)) \qquad (1)$$

Here, $Y_{J_j}(t)$ in Eq. (1) may be written as:

$$Y_{J_j}(t) = \sum_{i=1}^{M_{input}} W_{I_i J_j} X_{I_i}(t) \qquad (2)$$

Here, M_{input} is the input number and M_{hidden} is the unit number of the hidden layer. $X_{I_i}(t)$, ($i = 1,\ldots,M_{input}$) are input variables. $\left\{W_{I_i J_j}\right\}$ ($j = 1,\ldots, M_{hidden}$) and $\left\{W_{J_j K_1}\right\}$ are unknown synaptic weights between each layer. The function $f(Y_{J_j}(t))$ in Eq. (1) is defined by

$$f(Y_{J_j}(t)) = \frac{1}{1 + e^{-\alpha Y_{J_j}(t)}} \tag{3}$$

Where • is an unknown parameter.

To estimate the optimal values for unknown parameters $\theta = (N_L, \alpha, \{W_{I_iJ_j}\}, \{W_{J_jK_1}\})$, we minimized the following equation:

$$MSR(\theta) = \frac{1}{2N}\sum_{l=1}^{N}(R(l) - \tilde{R}(l\mid\theta))^2 + \frac{1}{2N_{1/3}}\sum_{j=1}^{N_{1/3}}(R_A(j) - \tilde{R}_A(j\mid\theta))^2 \tag{4}$$

Where N_L is the number of learning data, N is the number of estimating data and $N_{1/3}$ is the one-third numbers from top of all double amplitudes. $R(l)$ $(l=1,\ldots,N)$ is the measured value at time point j and $\tilde{R}(l|\theta)$ is the estimated value by the model. $R_A(j)$ and $\tilde{R}_A(j|\theta)$ $(j=1,\ldots,N_{1/3})$ are also the measured and the estimated value of the double amplitudes of the rolling motion, respectively. Then the *MSR* is defined as the weighted value between the mean squared residual of the estimation *MSE* and the mean squared residual of the significant double amplitude *MSEA*. To optimize θ, we used the modified back-propagation method based on the gradient descent algorithm as follow:

$$W^{(k+1)} = W^{(k)} - \eta \left.\frac{\partial E_p(W)}{\partial W}\right|_{W = W^{(k)}},$$

$$\eta = \begin{cases} 0.05 & (R_p > 0.0 \text{ and } \tilde{R}_p > R_p, \\ & \ R_p < 0.0 \text{ and } \tilde{R}_p < R_p) \\ 1.0 & (\text{otherwise}) \end{cases} \tag{5}$$

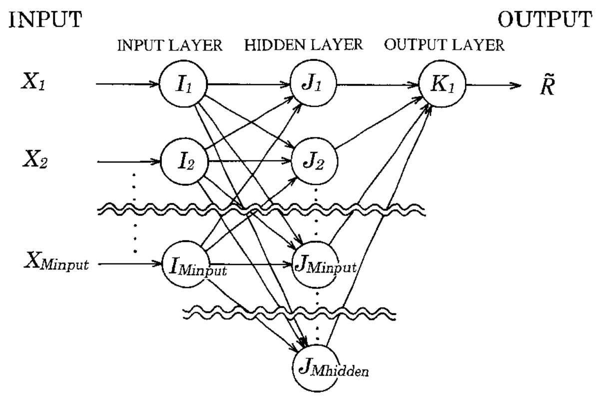

Fig.8. Structure of the multi-layered feed-forward network model

where $W^{(k)}$ is the connection weight at the kth iteration, and • is the step width of renewal varied in relation to the residual function $E_p(W)$ between the estimated rolling motion $\tilde{R}_p$ and the value of teacher signal R_p at the time point p [8].

3.2. Forecasting model of the rolling motion

In this paper, we adopted a recurrent *Neural Network* model in order to forecast the rolling motion. The model was added the feed back of the forecasting error to the feed-forward *Neural Network* model. Schematic diagram of structure of the model is shown in Fig. 9. As the feed back will vanish after learning, it looks the conventional feed-forward *Neural Network* model on the estimating shown in Fig. 8. The discrete recurrent *Neural Network* model is written as follow:

$$Y_{J_j}(t) = \sum_{i=1}^{M_{input}} W_{I_iJ_j}(\tau)X_{I_i}(t-\tau) + W_{I_{M_{input}+1}J_j}(\tau)X_{I_{M_{input}+1}}(t) \tag{6}$$

Where $X_{I_{M_{input}+1}}(t) = \left| R(t) - \tilde{R}(t) \right|$, • is time lag, $W_{I_iJ_j}(\tau)$ is the weight with time lag •.

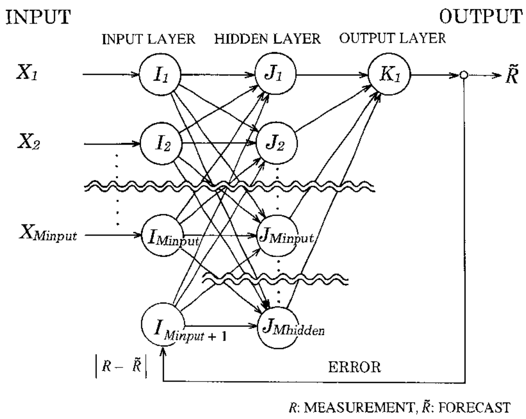

Fig.9. Structure of the recurrent network model on the learning stage

4. RESULT

4.1. Characteristics of the rolling motion

Let us investigate the time varying structure of each motion measured on the full-scale experiments. The first case is the 7.9 *GT* fishing vessel. Sea condition was right-bow waves with swell encountered from the right-guarter sea and the significant wave height $H_{1/3}$ was 0.74m. She moored her right side to the culture facilities with encountered the wave on the same side. The changes of spectra of the wave height, rolling motion and vertical mooring force for the facilities of the scallop culture for every 60 seconds, which correspond to 1200 samples, are shown in Fig. 10(a)-(c). Here, the horizontal, the longitudinal and the vertical axes indicate time(s), circular frequency • $(\mathrm{rad \cdot s^{-1}})$, and spectral density functions of the wave height S(•) $(\mathrm{m^2 \cdot s})$, the mooring force S(•) $(\mathrm{N^2 \cdot s})$ and the rolling motion S(•) $(\mathrm{deg^2 \cdot s})$, respectively. The measured time series can be regarded as stationary within the time interval. As for the wave height, it looks that the maximum value of the power largely changes although the dominant frequency slightly changes over time. On the other hand, in case of the vertical mooring force and the rolling motion, there are complicated powers in the wide frequency range. Then the features of spectra on the rolling motion and the mooring force are clearly different from those of the wave height.

The second case is the 6.6 *GT* fishing vessel. The mooring condition is different from the case of the 7.9 *GT* fishing vessel since the mooring side and encountering direction of the wave are opposite. It was reported that the roll response was complicated under such mooring condition [9]. In the experiment, wave was left-quartering and the significant wave height $H_{1/3}$ was 0.59m. The changes of spectra are shown in Fig. 11(a)-(c). Although mooring force itself is weak because the scallops are still small on the initial stage of the culture, there are powers in the low frequency range in addition to the existence of power on the same frequency range of the wave height. Time varying configuration of the power between the wave height and the rolling motion is different, even though the frequency range with the power is in almost same. It is regarded that the rolling motion is large nevertheless the wave height is small and the mooring force is weak.

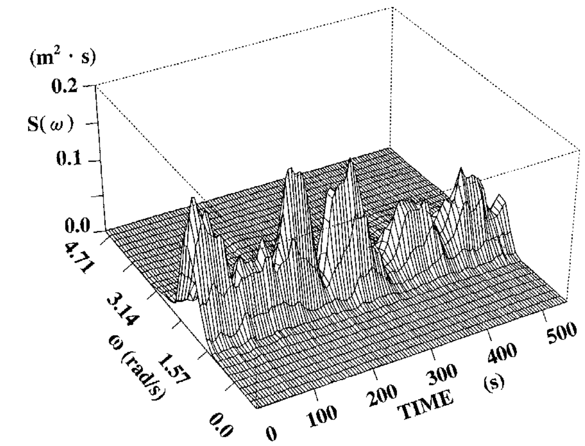

Fig. 10(a). Change of power spectra of the wave height, $H_{1/3}$ = 0.74m

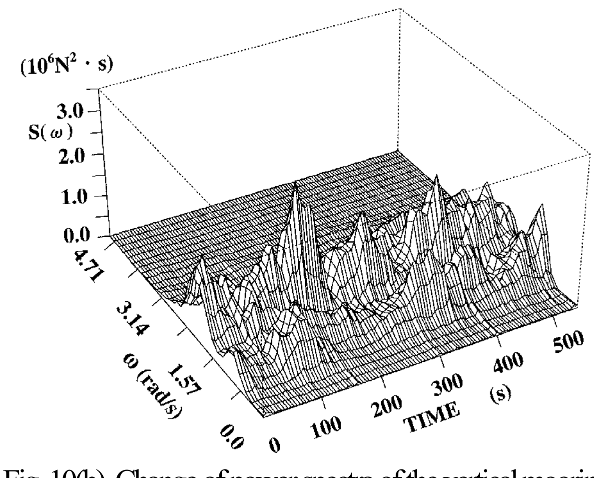

Fig. 10(b). Change of power spectra of the vertical mooring force on the 7.9 *GT* fishing vessel

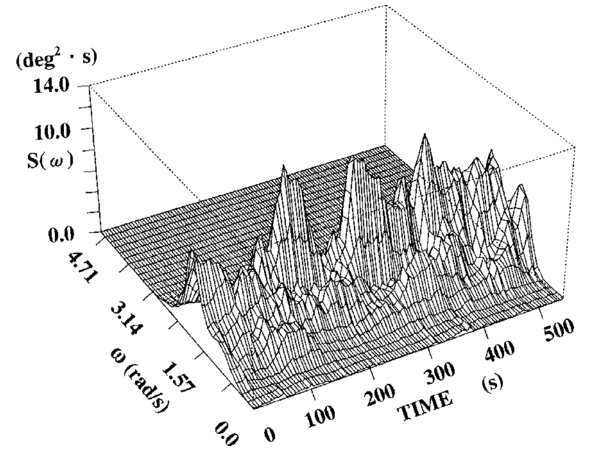

Fig. 10(c). Change of power spectra of the rolling motion on the 7.9 *GT* fishing vessel

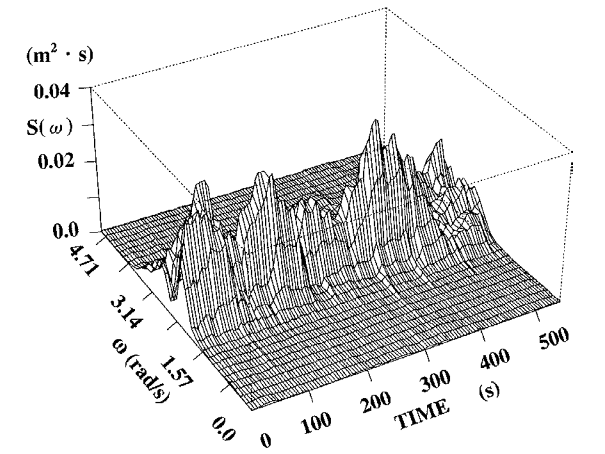

Fig. 11(a). Change of power spectra of the wave height, $H_{1/3}$ = 0.59m

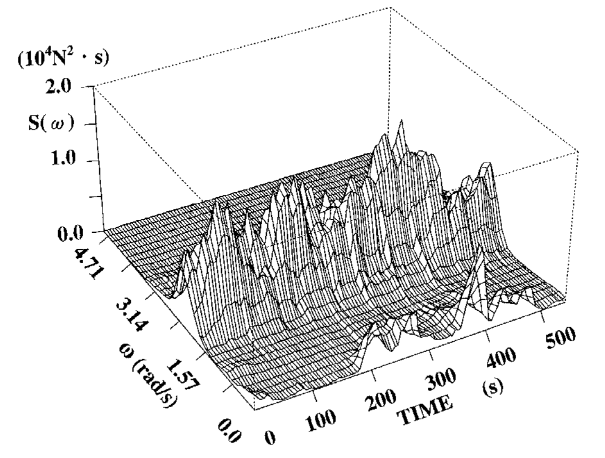

Fig. 11(b). Change of power spectra of the vertical mooring force on the 6.6 *GT* fishing vessel

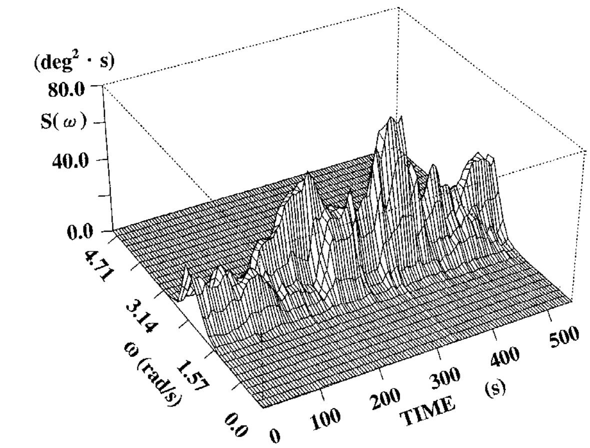

Fig.11(c). Change of spectra of the rolling motion on the 6.6 *GT* fishing vessel

4.2. Construction of the model and estimation of the roll response

Considering the movement of the ship on the sea, one of main input induced the rolling motion is the wave. To apply the *Neural Network* model to the rolling motion, we adopted five items (wave height, rolling, yawing and heaving motions, and vertical mooring force) as the input variables and the model expressed the effectiveness for the estimation of the roll response system [6-7]. Although wave height is essential to estimate the rolling motion, rational selection of the input is necessary to widely apply for the practical phenomenon. Then we conducted the restructuring of the model related to the proper input variables.

The accuracy of the estimation related to the input is shown in Table. 2. This is a result of the modeling for the actual measurement used the 7.9 *GT* fishing vessel shown in Fig. 10. To assess the accuracy of the estimation, *MSR* estimated by the model with the wave height is defined as the standard. Firstly, we tried to estimate the roll response only using the three variables: the vertical mooring force and the accelerations in Y and Z - directions measured at the center of gravity. Note that measured accelerations included the effect of the gravity according to the inclination. *MSR* is worse than the standard. In the case of the five variables that are added the accelerations in Y and Z - directions with time lag 1.40 seconds, which almost corresponds to the half natural rolling period of the ship (T_s = 2.91 seconds), *MSR* was considerably improved in comparison with that utilized

the wave height for the input. Then, we adopted the structure of the input to the model. An example on the estimation of the rolling motion is shown in Fig. 12. Where the solid line indicates the measured rolling motion and the dotted line indicates the estimation. The optimized parameters are •= 1.70 and M_{hidden} = 4. The estimation indicates enough accuracy related to the rolling motion at the inclining side acting the mooring force.
Another comparison with the accuracy is shown in Table 3. This is a result of the modeling for the experiment used the 6.6 *GT* fishing vessel shown in Fig. 11. Here, the natural rolling period of the ship T_s is 2.86 seconds. In the same result as the estimation of the 7.9 *GT* fishing vessel, it is clear that the model used the five variables on the input indicates proper estimation. An example on the estimation of the rolling motion is shown in Fig. 13. The optimized parameters are •= 0.94 and M_{hidden} = 3. It looks that the *Neural Network* model properly estimates the roll response structure because there is few underestimates. Note that the accelerations for the estimation were measured on the deck below the mooring point to the culture facilities since the model used the accelerations measured at the center of gravity could not estimate the rolling motion properly. In the conditions that the mooring force is weak, the model could not get the information related to the rolling motion from the accelerations measured at the center of gravity.

Table 2. Comparison with the accuracy of the estimation related to the input variables, 7.9 *GT* fishing vessel

INPUT VARIABLE	MSE	MSER	MSR
Mooring force, Acc-Y, Acc-Z	2.655	1.537	2.096
Mooring force, Wave, Acc-Y, Acc-Z	1.471	2.312	1.891
Mooring force, Acc-Y, Acc-Z, Acc-Y(7), Acc-Z(7)	1.812	1.290	1.551

Here, Acc-Y(7) and Acc-Z(7) are the accelerations in the Y and Z - directions with time lag corresponded to the half natural rolling period of the ship, respectively

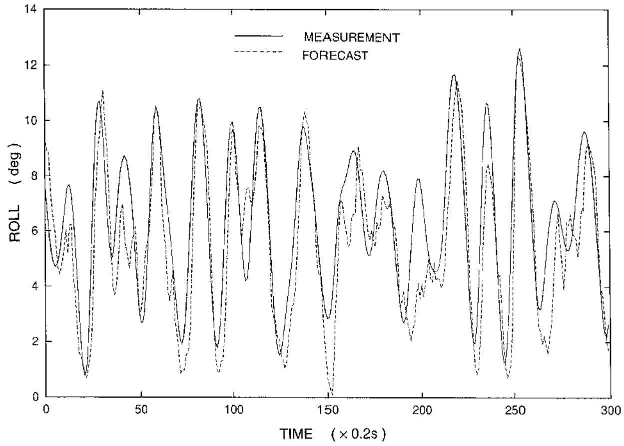

Fig.12. Estimation of the roll response on the 7.9 *GT* fishing vessel, •=1.70, M_{hidden} = 4 and *MSR* =1.551

Table 3. Comparison with the accuracy of the estimation related to the input variables, 6.6 *GT* fishing vessel

INPUT VARIABLE	MSE	MSER	MSR
Mooring force, Acc-Y, Acc-Z	4.886	2.288	3.587
Mooring force, Wave, Acc-Y, Acc-Z	4.423	1.638	3.030
Mooring force, Acc-Y, Acc-Z, Acc-Y(7), Acc-Z(7)	3.695	1.367	2.531

Here, Acc-Y(7) and Acc-Z(7) are the accelerations in the Y and Z - directions with time lag corresponded to the half natural rolling period of the ship, respectively

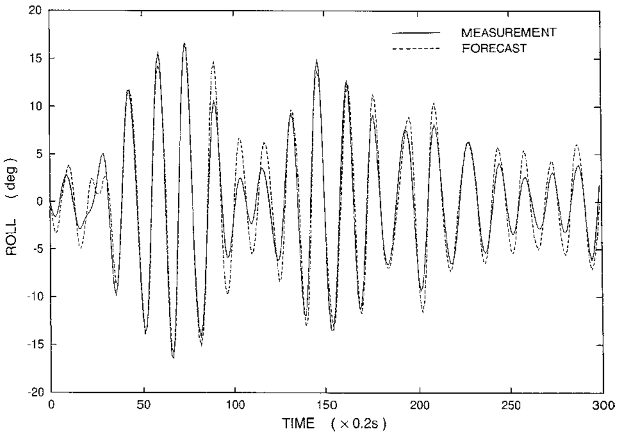

Fig.13. Estimation of the roll response on the 6.6 *GT* fishing vessel, •=0.94, M_{hidden} = 3 and *MSR* =2.531

4.3. Forecasting of the rolling motion by the recurrent *Neural Network* model

Two kinds of forecasting accuracies of the rolling motion by the recurrent *Neural Network* model with forecasting point ranging from 0 to 10 steps ahead are shown in Fig. 14 and Fig. 15, respectively. Here, one step of the forecasting point corresponds to 0.20 seconds. The input on the case shown in Fig. 14 is four variables: the mooring force, the wave height, and the accelerations in the Y and Z - directions. On the other hand, the input on the case shown in Fig. 15 is five variables: the mooring force, the accelerations in the Y and Z - directions, and the same accelerations with the half time lag of the natural rolling period. On the both cases, the forecasting accuracies of the rolling motion with the forecasting time ranging from 1.00 to 1.40 seconds are better than those of the estimation at the same time of the input. This time range getting nice accuracy of the forecasting corresponds to the half natural rolling period of the fishing vessel. Further, the forecasting accuracy on the case of four variables is almost equivalent to that on the case of five variables without the wave height. It means that the model can forecast the rolling motion only using the mooring force and the accelerations in the Y and Z - directions. An example on the forecasting of the rolling motion at six steps ahead is shown in Fig. 16. The optimized parameters are •=1.03 and M_{hidden} =5. Since there is few underestimating and time lag on the forecasting with *MSR* = 1.338, it looks that the recurrent *Neural Network* model properly forecasts the rolling motions under fishing operations. It is suggested that this non-deterministic model can be sufficiently applied to the practical rolling motion as the forecasting model.

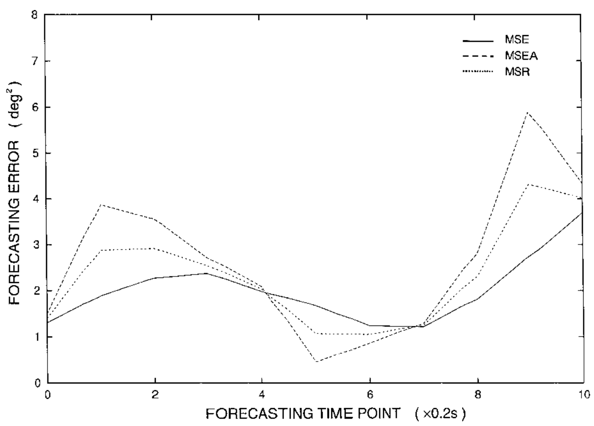

Fig.14. Forecasting error of the recurrent model with respect to the forecasting point, the input variables = 4

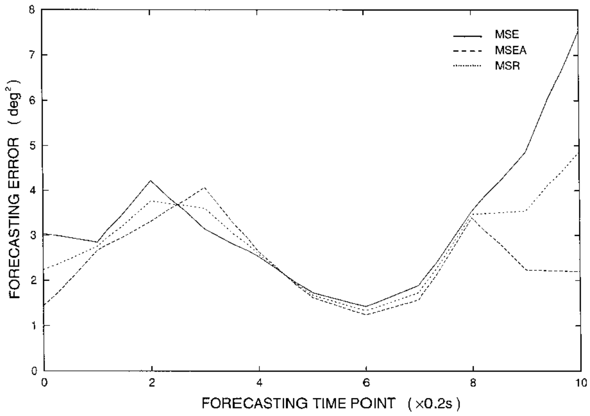

Fig.15. Forecasting error of the recurrent model with respect to the forecasting point, the input variables = 5

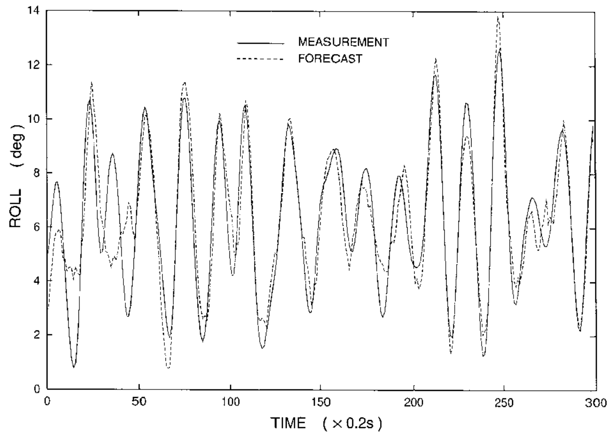

Fig.16. Forecasting of the rolling motion on the 7.9 *GT* fishing vessel at 6 steps ahead (1.20 second), •=1.03, M_{hidden} =5 and *MSR* = 1.338

5. CONCLUDING REMARKS

The conclusions in this study are summarized as follows:

1. On applying the feed-forward *Neural Network* model for the full-scale rolling motion under the fishing operation condition, it is confirmed that the non-deterministic model is practically effective to estimate the roll response system of the small fishing vessel acting the complicated outer force.

2. As the result of simplification related to the input variables, the roll response system could be estimated by only five variables as the input: the vertical mooring force, the accelerations in the Y and Z – directions and same accelerations with time lag corresponded to the half natural rolling period. Then, the estimated rolling motions are

independent on the wave height. It is suggested that the accelerations used for the estimation should be measured at the mooring point.

3. The recurrent *Neural Network* model can forecast the rolling motion under the fishing operation condition with sufficient accuracy. The input is five variables similar to the estimation of the rolling response system. The time range of forecasting is until the half period ahead of the natural rolling period of the fishing vessel.

6. ACKNOWLEDGEMENTS

The authors would like to express our thanks to Instructor T. Hokimoto and T. Iwamori of Hokkaido Univ. for the technical supports under the experiments.

7. REFERENCES

[1]. N. Kimura et al.: On the effectiveness of the forecasting for the rolling motion of a small fishing vessel using a neural network model, *Fishing Engineering*, 35(3), 234-161 (1999).

[2]. K. Amagai et al.: A study of the forecasting for the rolling motion of a small fishing vessel using a neural network model, *Fishing Engineering*, 34(2), 155-161 (1997).

[3]. M.Hamaguchi et al: A study on the characteristics of the rolling motion of a *135 GT* purse seiner during a fishing operation, *The Journal of Japan Institute of Navigation*,98,369-374 (1998).

[4]. T. Kodama et al.: A study of safety on fishing boats for scallop hanging type culture in mooring at trunk line, *The Journal of Japan Institute of Navigation*,100,221-227 (1999).

[5]. T. Kodama et al.: A study of safety on fishing boats for scallop hanging type culture in mooring at trunk line-II, *The Journal of Japan Institute of Navigation*,106,193-199 (2002).

[6]. N. Kimura et al.: Estimation of dynamic rolling response of small fishing vessels in fishing operations using a neural network model, *7th international conference on stability of ships and ocean vehicles*,861-867(b) (2000).

[7]. N. Kimura et al.: Non-deterministic approach for the movement of small fishing vessels, Fisheries Science, 68, 1823-1826 (2003).

[8]. N. Kimura et al.: A method for estimating nonlinear rolling of small fishing boats, *4th Osaka Colloquium on Seakeeping Performance of Ships*, 451-458 (2000).

[9]. K. Izutsu et al.: A study of the relation between encountered wave and roll response during operation of the scallop culture small fishing boats, *The Journal of Japan Institute of Navigation*, 104,117-124 (2001).